

Dissolution and Hydrolysis of Cellulose in Subcritical and Supercritical Water

Mitsuru Sasaki, Zhen Fang, Yoshiko Fukushima, Tadafumi Adschiri, and Kunio Arai*

Department of Chemical Engineering, Faculty of Engineering, Tohoku University, 07 Aza-Aoba, Aramaki, Aoba-Ku, Sendai, Miyagi 980-8579, Japan

Decomposition experiments of microcrystalline cellulose were conducted in subcritical and supercritical water (25 MPa, 320–400 °C, and 0.05–10.0 s). At 400 °C hydrolysis products were mainly obtained, while in 320–350 °C water, aqueous decomposition products of glucose were the main products. Kinetic studies of cellulose, cellobiose, and glucose at these conditions showed that below 350 °C the cellulose decomposition rate was slower than the glucose and cellobiose decomposition rates, while above 350 °C, the cellulose hydrolysis rate drastically increased and became higher than the glucose and cellobiose decomposition rates. Direct observation of the cellulose reaction in high-temperature water at high-pressure conditions by using a diamond anvil cell (DAC) showed that, below 280 °C, cellulose particles became gradually smaller with increasing reaction time but, at high temperatures (300–320 °C), cellulose particles disappeared with increasing transparency and much more rapidly than expected from the lower temperature results. These results suggest that cellulose hydrolysis at high temperature takes place with dissolution in water. This is probably because of the cleavage of intra- and intermolecular hydrogen linkages in the cellulose crystal. Thus, a homogeneous atmosphere is formed in supercritical water, and this results in the drastic increase of the cellulose decomposition rate above 350 °C.

Introduction

Biomass is an important resource that can be converted to energy, chemicals, foods, and feedstocks. For example, cellulose, which is a main component of the biomass, can be applied to various industries of papers, fiber, foods, and chemicals. Cellulose oligomers, which are the hydrolysis products of cellulose, are also useful ingredients for medicines.

Cellulose is a homopolymer, in which 100 to 3000 glucose residues are straightly combined with each other at the $\beta(1,4)$ position. Each glucose residue has three hydroxyl groups, and therefore it has a high affinity to water. Thus, basically cellulose molecules may be dissolved in water. However, because of their intermolecular and intramolecular hydrogen linkages through the hydroxyl groups, cellulose molecules form crystal structures at normal conditions.

In recent years, several researchers reported that hydrolysis takes place for ether or ester bonds in near-critical or supercritical water ($T_c = 374.2$ °C; $P_c = 22.1$ MPa; $\rho_c = 323.2$ kg/m³) in the absence of catalysts.^{1–6} Malaluan thought that the noncatalytic hydrolysis in near-critical or supercritical water could be applied for the conversion of waste biomass to various chemicals and started research on cellulose hydrolysis.⁷ A flow-type microreactor with a HPLC pump was used for the cellulose decomposition experiments. It was found that the cellulose decomposition rate in supercritical water was extremely fast and the hydrolysis products of cellulose could be produced in relatively high yield.⁷ Kinetic studies for the reactions of cellulose and cel-

lulose-related compounds (glucose and cellobiose) in subcritical and supercritical water were also conducted. In the range of temperature from 300 to 350 °C, the cellulose hydrolysis rate showed a straight relationship to the reciprocal temperature. On the contrary, at 400 °C, the reaction rate was 1 or 2 orders of magnitude higher than that in subcritical temperature.⁷

However, Malaluan could not conduct a more detailed study because of the difficulty in feeding cellulose–water slurries using the HPLC pump.⁷ Recently, we developed a slurry feeder which could continuously supply cellulose–water slurries (20 wt %). The flow reactor with this slurry feeder enabled us to study the cellulose hydrolysis in subcritical and supercritical water in more detail. As a result, we found that the cellulose decomposition rate increased substantially around the critical temperature and that the hydrolysis products yield increased drastically with increasing temperature.⁸

In this study, to evaluate the drastic change of the cellulose hydrolysis rate and product distributions around the critical temperature in more detail, we conducted cellulose decomposition experiments in the range of temperatures from 320 to 400 °C. Also, we performed the direct observation of the cellulose–water reaction field with a diamond anvil cell (DAC) for high-temperature and high-pressure conditions.

Experimental Section

Materials. Cellulose used was de-ashed microcrystalline cellulose (Avicel No. 2331; average particle diameter 20–100 μ m) purchased from Merck. The reagents used for HPLC analysis are as follows: cellobiose (99+%), cellotriose (95+%), cellotetraose (95+%),

* To whom correspondence should be addressed. Phone/Fax: +81-22-217-7246. E-mail: karai@arai.che.tohoku.ac.jp.

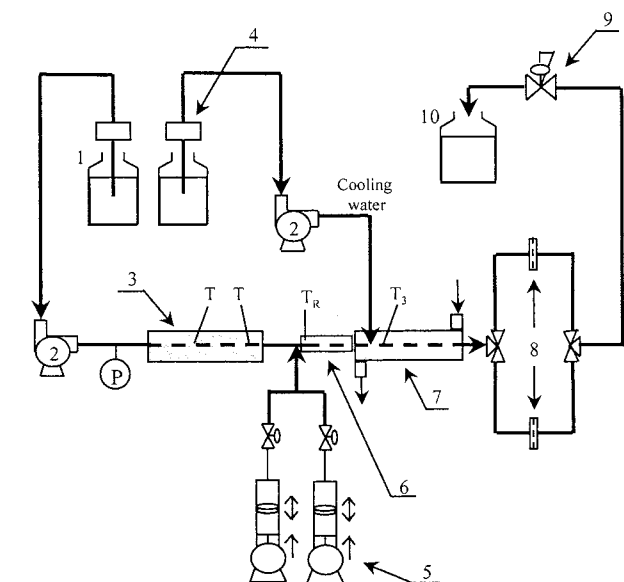


Figure 1. Schematic diagram of the experimental setup: (1) distilled water storage; (2) high-pressure pump; (3) electric furnace; (4) degassing unit; (5) slurry feeder; (6) reactor; (7) cooling water jacket; (8) in-line filters; (9) backpressure regulator; (10) sampling bottle.

cellopentaose (95+%), and cellohexasose (95+%) (Seikagaku Industrial Co. Ltd. (Tokyo)); glucose (99+%), fructose (99+%), erythrose (60+%), dihydroxyacetone (99+%), 1,6-anhydroglucose (99+%), glyceraldehyde (97+%), pyruvaldehyde (40%), 5-(hydroxymethyl)-2-furaldehyde (60+%), and furaldehyde (80%) (Wako Pure Chemicals Industries Ltd. (Osaka)).

Cellulose Decomposition Experiments and Product Analyses. Cellulose decomposition experiments were conducted at temperatures ranging from 320 to 400 °C, a pressure of 25 MPa, and residence times of between 0.05 and 10.0 s.

A flow-type reactor with a specially designed slurry feeder was used in cellulose decomposition experiments. A schematic diagram of this apparatus is shown in Figure 1. The slurry feeder has two slurry tanks of 300 mL, the inside of which is stirred by a mixer externally propelled by a permanent magnet. Cellulose–water slurries (10 wt %) were loaded in the slurry tank and stirred for 30–60 min prior to the experiment. The slurry was fed to the reactor at a flow rate of 5.0 mL/min and mixed with preheated water fed from the other line at a flow rate of 20.0 mL/min. The concentration of cellulose–water slurries after the mixing point was about 2 wt %. At the mixing point, the slurry was rapidly heated to the reaction temperature, T_R (320–400 °C). The reaction temperature (T_R) in the reactor was measured by a thermocouple at 2 cm after the mixing point, as shown in Figure 1. For the case that the temperature could not be measured because we conducted these decomposition experiments at very short residence times, we evaluated the reaction temperature from the enthalpy balance, instead of measuring the reaction temperature. In this evaluation, the difference of the temperature measured and the temperature evaluated from the enthalpy balance was ± 2 °C. At the exit of the reactor, to terminate the reaction rapidly, cooling water was introduced directly into the system at a flow rate of 8.0 mL/min. At the same time, this part was externally cooled by a cooling water jacket. The reaction volume (V) could be accurately determined

by this rapid-heating and quick-quenching method. The residence time (τ) in the reactor was evaluated by eq 1,

$$\tau = \frac{V\rho(P,T)}{F\rho} \quad (1)$$

where ρ is the density of a fluid mixture and is assumed to be a pure water density in this study because of the lower concentration of cellulose (about 2 wt %).

The reaction pressure of this system was controlled by a backpressure regulator (TESCOM model 26-1721-24). The product solution was filtered with in-line filters (NUPRO SS-4TF-05) of 0.5 μm pore size and continuously recovered through the backpressure regulator in a sampling bottle.

The aqueous products were analyzed by ^1H nuclear magnetic resonance (^1H NMR) and fast atom bombardment mass spectroscopy (FAB-MS).⁷ They were also analyzed for the total organic carbon (TOC) by a TOC analyzer (Shimadzu model TOC-5000A), and their compositions were quantified by high-performance liquid chromatography (HPLC). In some cases, we observed that the white precipitates appeared in the product solution. Therefore, the liquid products were first submerged in the cool water bath kept at 20 °C for 2 h and then incubated in an air bath at a constant temperature of 20 °C for 2 days. If the white precipitates were formed in the liquid solution, they were filtered, washed with water several times, and dried at 60 °C for 24 h. The dried precipitates were weighed and analyzed by FTIR in order to identify the macromolecular structures of the precipitates. On the contrary, the filtrated aqueous products were analyzed by TOC and HPLC–UV/RI in order to quantify their compositions.

The HPLC equipment consisted of an isocratic pump, an autosampler, and an integrator (Thermoquest models P1000, AS3000, and SP4400, respectively). The column used for the analysis was a SUGAR KS-801 (Shodex). The HPLC was operated at an oven temperature of 80 °C with 1.0 mL/min flow of the water solvent. The detectors used were an ultraviolet detector (UV; Thermoquest model Spectra 100) set at 290 nm and a refractive index detector (RI; ERC model 7515A). The RI detector provided quantitative analysis, while the UV detector was used to confirm the presence or absence of compounds with double bonds such as C=O and C=C in the products. Peak identification was established by comparison of the sample peak retention times with the standard solution of the pure compound. The calibration of the peaks was performed using standard solutions of varying concentrations to develop a linear relationship between the peak area and the corresponding concentration.⁹

Solid residues trapped in the in-line filters for 30 min were dried at 60 °C for 24 h after the experiment and weighed (W). These residues were also analyzed by FTIR, XRD, and SEM.

Cellulose conversion (X) was evaluated by eq 2 as

$$X = \frac{W_0 - W}{W_0} \quad (2)$$

where W_0 is the total amount of cellulose introduced for 30 min and W is the amount of cellulose recovered after the experiment.

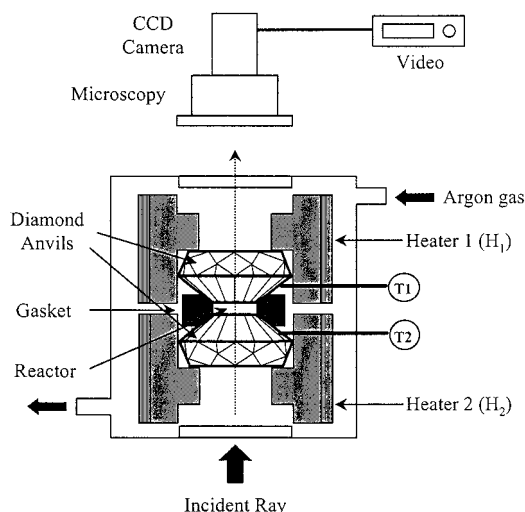


Figure 2. Experimental apparatus of the DAC.

The product yield (Y_i) and product selectivity (S_i) were defined as

$$Y_i = \frac{W_i}{W_0} \quad (3)$$

$$S_i = \frac{Y_i}{X} \quad (4)$$

where W_i , Y_i , and S_i are the weight, the product yield, and the product selectivity of component i , respectively.

Direct Observation of the Cellulose–Water Reaction Field. For the direct observation of the cellulose–water reaction field, the DAC, which was developed by Bassett et al.,¹⁰ was used. Figure 2 shows the schematic diagram of this apparatus. A rhenium (Re) gasket was sandwiched between two diamonds and the enclosed space within the gasket (0.5 mm i.d., 0.25 mm thickness), and the diamonds were used as reactors. A cell temperature was controlled by two heaters and thermocouples attached to the diamond windows and recorded with a temperature acquisition board (Hewlett-Packard model 37970A). The reaction temperature in the hole of the gasket was evaluated as the average of the two temperatures (T_1 and T_2). To prevent oxidation of the diamonds, argon gas with 1.0% hydrogen was introduced into the cell.

First, a ruby chip and cellulose particles are introduced into the gasket hall on the lower diamond. Then, water is loaded into the gasket hole with a microsyringe. They are enclosed in the cell by installing the upper diamond anvil. Finally, the heaters (H_1 and H_2) and thermocouples (T_1 and T_2) are connected in preparation for heating, while the sample is observed at 100 times of magnification and the images are recorded with a CCD camera (Olympus KY-F55MD, Tokyo) system. The initial pressure in the cell was evaluated from the shifts of the fluorescence of the enclosed ruby. However, because of the experimental limitation (batch-type experiments), the pressure of the system at reaction conditions could not be controlled and monitored. Complete details on the experimental procedure and method are described in a previous publication.¹¹ In this study, the behavior of cellulose particles was observed for 30 min at 190, 210, 230, and 250 °C. An experiment with a constant heating rate (10 K/s) from 250 to 400 °C was also conducted.

Table 1. Chemical Species Detected in Cellulose Decomposition Experiments

products detected	analytical method
Hydrolysis Products	
higher DP materials (water-insoluble)	IR, quantitative anal. ^a
cellohexaose	HPLC, FAB-MS ^b
cellopentaose	HPLC, FAB-MS ^b
cellotetraose	HPLC, FAB-MS ^b
cellotriose	HPLC, FAB-MS ^b
cellobiose	HPLC, FAB-MS ^b
glucose	HPLC, ¹ H NMR ^c
fructose	HPLC, ¹ H NMR ^c
Aqueous Decomposition Products of Glucose and Fructose	
1,6-anhydroglucose	HPLC, ¹ H NMR ^c , traces
erythrose	HPLC, ¹ H NMR ^c
glycolaldehyde	¹ H NMR ^c
glyceraldehyde	HPLC, ¹ H NMR ^c
dihydroxyacetone	HPLC, ¹ H NMR ^c
pyruvaldehyde	HPLC, ¹ H NMR ^c
5-(hydroxymethyl)-furaldehyde (5-HMF)	HPLC
furaldehyde	HPLC

^a Saeman, J. F.; et al. *Ind. Eng. Chem.* **1945**, 37 (1), 43.

^b Malaluan, R. M. Ph.D. Dissertation, Tohoku University, Sendai, Japan, 1995. ^c Kabyemela, B. M. Ph.D. Dissertation, Tohoku University, Sendai, Japan, 1998.

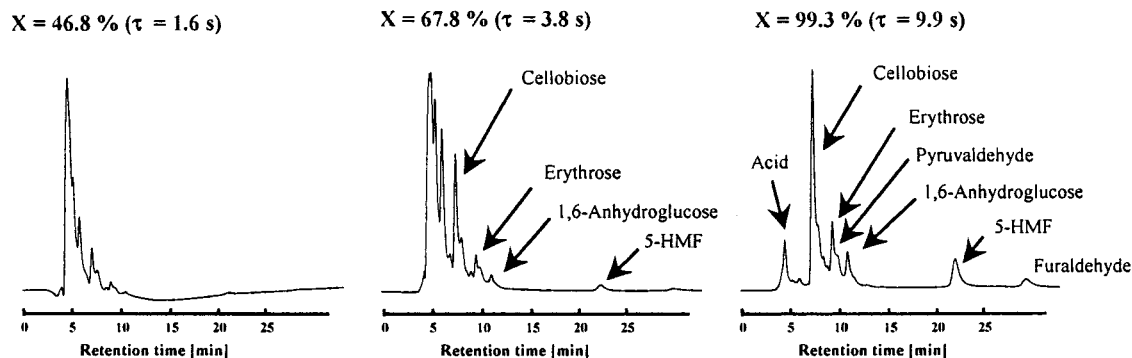
Results

Cellulose Decomposition Product Distribution.

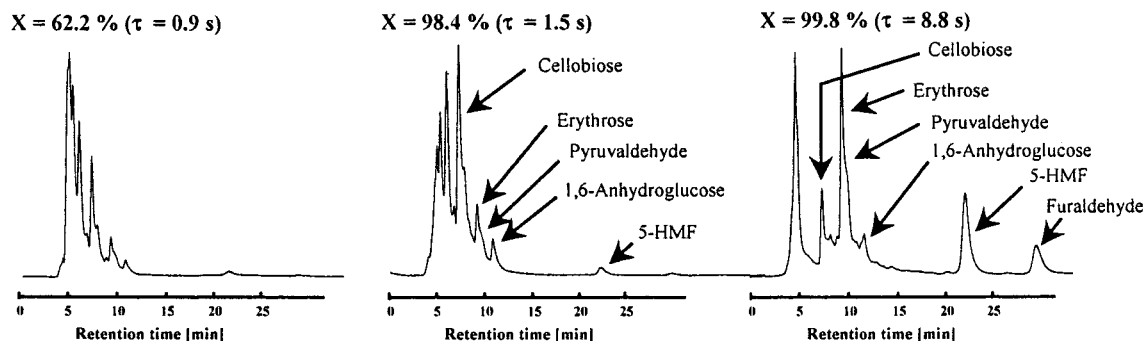
The cellulose decomposition products identified and quantified in the experiments are shown in Table 1. The main products are aqueous oligomers (cellohexaose, cellopentaose, cellotetraose, cellotriose, and cellobiose), monomers (glucose and fructose), and aqueous decomposition products of glucose (1,6-anhydroglucose, glyceraldehyde, erythrose, glycolaldehyde, dihydroxyacetone, pyruvaldehyde, 5-(hydroxymethyl)-2-furaldehyde (5-HMF), furaldehyde, and acids). In this study, we defined the combination of oligomers and monomers as the "hydrolysis products". Though furaldehyde was identified, it was not quantified. With regard to the peak at low retention time in the HPLC chromatogram, several compounds such as aldehydes, alcohols, and carbonic acids were supposed to be included. Holgate et al. conducted glucose decomposition experiments in supercritical water (425–600 °C and 246 bar) and reported the formation of acetic acid and lactic acid¹² as the main products. We also conducted the product analyses for lower molecular weight products by GC–FID and GC–MS. The results indicated that the main components of the lower molecular weight products are acetic acid and formic acid. The yields of lactic acid, acrylic acid, and other species were much lower than those of these acids. Therefore, we tried to evaluate the yield of the organic acids by using the pH value of the aqueous solution. In this case, we assumed the carbon number and the acid dissociation constant (pK_a) of the solution to be 1.5 and 4.0, respectively, and then calculated the yield of organic acids, because the acid dissociation constants of acetic acid (C_2) and formic acid (C_1) are 4.55 and 3.56, respectively. In these calculations, the total carbon balance in each experiment was satisfactory (95–100%).

The HPLC chromatograms of the products at temperatures of 320, 350, and 400 °C, which is set at 25 MPa, are shown in Figure 3a–c, respectively. The product distributions are also shown in Table 2. At a temperature of 320 °C, cellulose conversion at 1.6 s was

(a) 320 °C



(b) 350 °C



(c) 400 °C

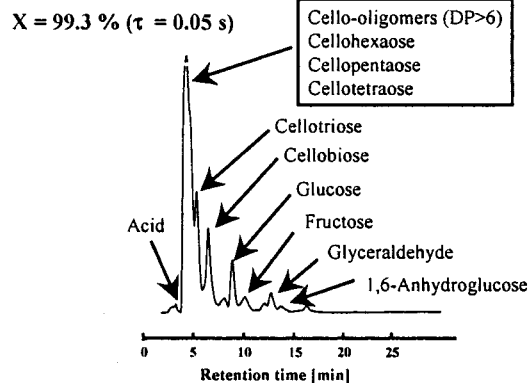


Figure 3. HPLC chromatograms of recovered liquid samples: (a) 320 °C; (b) 350 °C; (c) 400 °C.

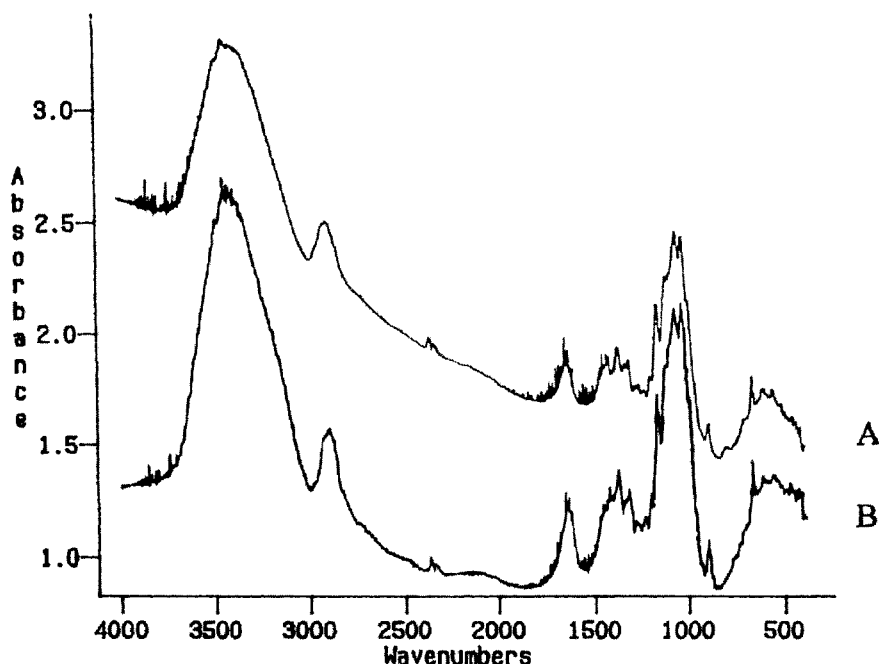
46.8%. The yield of hydrolysis products (cellobiose, glucose, etc.) was 43.9%, and the yield of aqueous decomposition products of glucose was 2.9%. In this case, cellulose conversion decreased when the residence time (τ) increased from 1.6 to 2.5 s. This is an experimental error. At a residence time of 3.8 s, the conversion increased to 67.8%. The yield of hydrolysis products reached 53.6%, and the yield of aqueous decomposition products of glucose was 14.2%. In the case of 9.9 s, the cellulose conversion reached approximately 100%. Under these conditions, the yield of hydrolysis products declined to 14.7% and the yield of aqueous decomposition products of glucose increased up to 84.6%. Also, char was formed as a residue in this condition. In the case of 350 °C, cellulose conversion was 62.2% at a residence time of 0.9 s. The yield of hydrolysis products was 50.2% (oligomers, 45.6%; monomers, 4.6%), while the yield of aqueous decomposition products of glucose

was 12.0%. At the residence time of 3.5 s, cellulose conversion reached 99.5%. Under this condition, the yield of hydrolysis products decreased to 27.0% and the main products were monomers (25.3%). The yield of aqueous decomposition products of glucose also increased to 72.5%. By comparison of the product distributions at 320 and 350 °C, it is suggested that the reactions of 320 and 350 °C proceeded with a similar mechanism, because similar product distributions were obtained at 320 and 350 °C. These results shown here clearly indicate that hydrolysis products (oligomers and monomers) further decomposed to aqueous decomposition products of glucose, including glyceraldehyde, erythrose, dihydroxyacetone, pyruvaldehyde, 1,6-anhydroglucose, 5-HMF, and furaldehyde, when the cellulose conversions reached 100% at 320 and 350 °C.¹³ On the contrary, at 400 °C, the cellulose conversion reached approximately 100% at the short residence time (0.05

Table 2. Product Distribution of Cellulose Decomposition in Subcritical and Supercritical Water

<i>t</i> [s]	conv [%]	product yield [C %]												
		hydrolysis products						aqueous decomposition products of monomers ^c						
		oligomers ^a				monomers ^a								
		>6	4–6	CT	CB	Glc	Fru	GA	DA	AG	Ery	PA	HMF	acids
(a) Temperature 320 °C, Pressure 25 MPa														
1.6	46.8	25.2	11.1	5.2	0.5	1.5	0.4	0.7	0.4	0.3	0.9	0.4	0.1	0.1
2.5	43.1	11.3	19.3	0.1	4.2	2.2	1.5	0.5	0.3	0.6	1.1	0.9	0.2	0.9
3.8	67.8	n.d.	30.6	0.1	9.0	10.4	3.5	1.1	0.3	1.8	2.3	2.0	0.8	5.9
7.3	97.7	n.d.	3.0	0.1	3.7	19.7	3.0	1.9	0.5	6.2	7.0	3.2	5.0	44.4
9.9	99.3	n.d.	0.7	0.1	0.4	7.6	5.9	11.0	0.3	6.2	4.2	0.2	9.3	53.4
(b) Temperature 350 °C, Pressure 25 MPa														
0.9	62.2	14.0	18.8	10.8	2.0	3.8	0.8	3.6	0.3	0.1	1.4	1.1	0.8	4.7
1.5	98.4	10.1	17.6	18.7	4.2	9.8	1.9	9.4	0.4	0.1	3.2	5.6	1.7	15.8
3.5	99.5	n.d.	0.3	0.1	1.3	24.8	0.5	2.8	0.7	8.1	9.4	6.2	6.1	39.2
8.8	99.3	n.d.	0.3	0.1	0.4	1.6	1.9	14.2	0.3	3.0	5.1	0.9	10.9	60.6
(c) Temperature 400 °C, Pressure 25 MPa														
0.01	99.0	51.0	12.3	0.5	8.4	2.3	2.0	1.9	4.8	2.8	8.6	4.3	0.1	6.1
0.05	98.6	0.2	14.2	1.2	11.7	24.2	13.2	12.2	0.3	4.9	6.5	0.3	0.4	10.7
0.15	99.8	n.d.	5.3	0.1	9.1	9.6	33.0	17.6	0.4	5.7	8.2	0.3	1.1	10.4

^a Oligomers are divided into two parts: one is the “aqueous oligomers” (cellobiose, cellotriose, cellotetraose, cellopentose, and cellohexaose), and the other is “water-insoluble oligomers” (the white precipitates). ^b Monomers: glucose and fructose. ^c Monomer decomposition products: 1,6-anhydroglucose, erythrose, glycolaldehyde, glyceraldehyde, dihydroxyacetone, pyruvaldehyde, 5-HMF, and acids. The yield of acids was calculated by the pH value of the solution.

**Figure 4.** IR spectra of the original cellulose (A) and the precipitate treated at 400 °C, 25 MPa, and 0.16 s (B).

s). An interesting point is that hydrolysis products were mainly obtained at 0.01–0.05 s (the yield of hydrolysis products, 65–77%) even at extremely high conversions (98–100%). These results suggest that the reaction atmosphere at 400 °C is totally different from that at 320 and 350 °C.

Precipitation Products. Aqueous products obtained in the experiment around the critical temperature were clear transparent liquid solutions right after the experiment. However, white precipitates appeared in the solution after cooling for 30 min to 2 h at 20 °C. Even for 320 and 350 °C, though the precipitates also appeared at short residence time, its amount was very small.

The precipitate obtained was dried at 60 °C for 24 h and analyzed by FTIR. As shown in Figure 4, the IR spectrum of the precipitates was more or less the same

as that of the original cellulose. When the precipitates were hydrolyzed in a dilute sulfuric acid aqueous solution (4.0%) for 240 min at 30 °C, they dissolved and then hydrolyzed to glucose. These results indicated that the precipitates were high degree of polymerization (DP) oligomers that have cellulose-like molecular structure.

The above results suggest that the hydrolyzed oligomers that still had high DPs and thus were insoluble in water at low temperatures were solubilized in high-temperature water during the reaction at 400 °C but recrystallized by cooling at 20 °C for 30 min to 2 h.

Cellulose Decomposition Rate in Subcritical and Supercritical Water. We conducted FTIR measurements and SEM observations of solid residues recovered after the experiments in subcritical water. These analyses suggested that solid residues have almost the same macromolecular structure as the

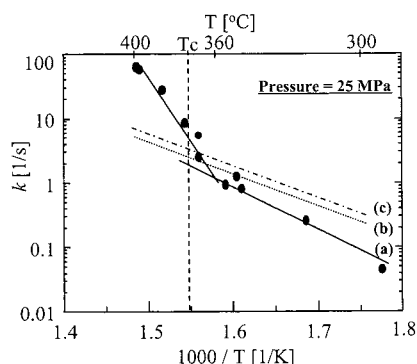


Figure 5. Arrhenius plot of the decomposition rate constants of cellulose and related cellulosic compounds in subcritical and supercritical water: (a) cellulose; (b) cellobiose;¹⁴ (c) glucose.⁹

original cellulose and their average particle sizes grew gradually smaller with residence time. Moreover, the XRD analysis showed that the solid residues have remained the crystal structure of the original cellulose. The above results suggest that the solid residues are cellulose. Thus, we evaluated the first-order rate constant of cellulose decomposition from the conversion of cellulose (X), by eq 5.

$$k = -\frac{\ln(1 - X)}{\tau} \quad (5)$$

The evaluated first-order rate constant (k) was plotted against reciprocal temperature in Figure 5. Below 350 °C, the Arrhenius plot gave a straight line. Above 350 °C, however, the reaction rate drastically increased, and at 400 °C, it was more than 1 order of magnitude higher than the rate at 350 °C. This suggests that the reaction mechanism changed around 350 °C.

The decomposition rates of glucose and cellobiose, both of which are the hydrolysis products of cellulose, evaluated in our previous works^{9,14} are also shown in this figure. At a lower temperature region, both glucose and cellobiose conversion rates were much faster than the hydrolysis rate of cellulose. However, as a result of the increase of the cellulose hydrolysis rate above 350 °C, at 400 °C it became much faster than the conversion rates of glucose and cellobiose.

Direct Observation by DAC. Direct Observation of the Reaction Field and Evaluation of the Shrinking Rate of Cellulose Particles. The direct observation experiments of cellulose in high-temperature water were performed by using the DAC. Because of the experimental limitation of DAC (batch type), the system pressure could not be controlled and monitored. At 190, 210, 230, and 250 °C, cellulose particles became gradually smaller with increasing reaction time. A shrinking rate constant (k_s) at 190–250 °C was calculated from the change of the particle length by eq 6 where t is the

$$k_s = \frac{\frac{1}{n} \sum_{i=1}^n (L_{i,0} - L_i)}{2t} \quad (6)$$

observation time [min], n is the number of cellulose particles which are used on this calculation, $L_{i,0}$ is the initial particle size of cellulose particle i [μm], and L_i is the particle size of cellulose particle i at t [μm]. The shrinking rate constants evaluated are shown in Figure 6. Cellulose shrinking rate constants at temperatures

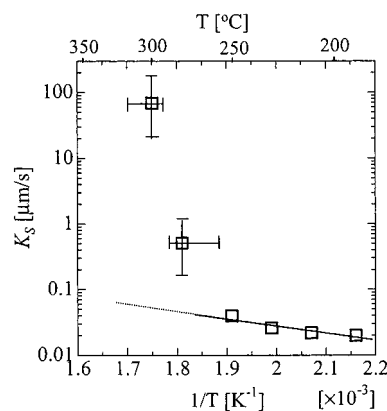


Figure 6. Arrhenius plot of the shrinking rate constants of cellulose particles. The initial pressure of the DAC at room temperature is 60 MPa.

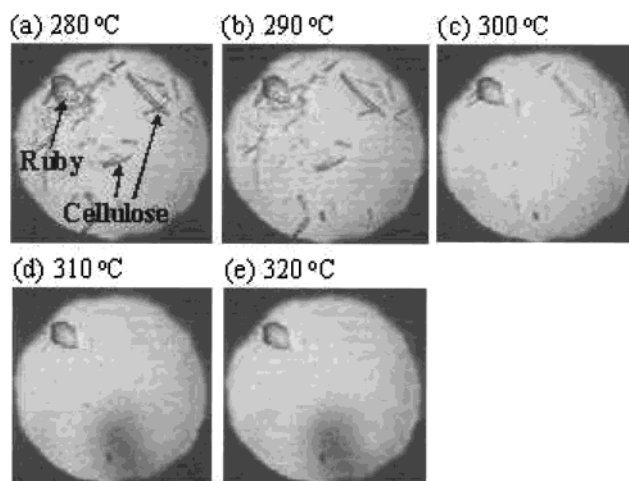


Figure 7. DAC study of cellulose in water at 280–320 °C (the initial pressure at room temperature, 60 MPa). Conditions: (a)–(e) photographs at approximately 1 s intervals with heating from 280 °C at a heating rate of 10 K/s. Diameter of the Re gasket hole is 0.5 mm with a thickness of 0.25 mm. Ruby is for pressure measurement.

of 190, 210, 230, and 250 °C showed a linear relationship with reciprocal temperature.

At a higher temperature range, the effect of shrinkage during the heating period is so significant that shrinking rates at constant temperatures could not accurately be evaluated. Thus, an experiment with a constant heating rate (10 K/s) up to 400 °C was conducted and the average shrinking rates in the higher temperature ranges were evaluated. Typical examples of the observation results are shown in Figure 7a–e. At higher temperatures (300–320 °C), cellulose particles disappeared with increasing transparency. Average shrinking rates in the range from 250 to 280 °C and that from 280 to 320 °C evaluated were plotted with error bars at 265 and 300 °C in Figure 6. The average shrinking rate at 300 °C significantly deviated from the straight line and became more than 2 orders of magnitude higher than that estimated by the extrapolation from the lower temperature data (see a dashed line in Figure 6).

Discussion

At the lower temperature region (below 350 °C), the main products were the aqueous degradation products of glucose, namely, erythrose, glyceraldehyde, dihydroxyacetone, pyruvaldehyde, 1,6-anhydroglucose, 5-HMF,

furfural, and acids. However, at 400 °C, most of products obtained were hydrolysis products, including monomers (glucose and fructose) and oligomers (cellohexaose, cellopentaose, cellotetraose, cellotriose, and cellobiose). This difference can be explained by the change in the cellulose hydrolysis rate and the decomposition rates of glucose and cellobiose. Below 350 °C, glucose or cellobiose decomposition rates were much faster than that of the cellulose hydrolysis rates. This is the reason for the high yield of aqueous degradation products of glucose under the conditions. However, around 350 °C the cellulose hydrolysis rate drastically increased and at 400 °C became much faster than the decomposition rates of glucose and cellobiose. This is the reason we obtained a high yield of hydrolysis products at 400 °C. Next, the reason for the increase of the hydrolysis rate at around 350 °C is discussed below.

We found that liquid products obtained in the experiment around the critical temperature (especially at 400 °C) were transparent just after the experiment but that the high-DP oligomers appeared in the solution after 2 h to 2 days as white precipitates. The direct observation of the reaction field at high-temperature water showed that cellulose disappeared with increasing transparency at around 300–320 °C, while the cellulose particle size became small gradually at below 250 °C. The average shrinking rates at around 265 and 300 °C were much faster than that at the lower temperature range of 190–250 °C.

These results suggest the change of the reaction mechanism at higher temperatures. We think one reason for the change of the cellulose disappearance rate at high temperature is the dissolution of cellulose or hydrolyzed oligomers that still have high DPs in high-temperature water, which leads to the formation of a homogeneous hydrolysis atmosphere. Because of the intramolecular and intermolecular hydrogen linkages, cellulose is in the form of crystal under normal conditions. As the reaction temperature increases high enough to break hydrogen linkages in crystals of cellulose, the cellulose crystal might disperse into high-temperature water and forms a homogeneous cellulose–water reaction atmosphere.

However, the break point of the cellulose disappearance rate (350 °C) was different from that observed by the DAC experiment (300–320 °C by sight or 250–260 °C from the shrinking rate). Although we do not have a clear explanation for the difference of the break points at the moment, possible reasons are considered to be (1) the mixing or heat-transfer rate effect at the mixing region where high-temperature water and cellulose–water slurries encounter one another, (2) the difference of the reaction atmosphere between the DAC experiment and the flow type experiment, and (3) the experimental errors for monitoring the reaction temperature on the DAC experiments. Especially, for the experimental condition, the water density of the reaction atmosphere was significantly different between the two experiments. In the DAC experiment, the water density in the cell was around unity even at higher temperature, while for a flow-type experiment, it was around 0.74 g/mL at 300 °C and 25 MPa and around 0.17 g/mL at 400 °C and 25 MPa. The dielectric constant of water at 300 °C and at a density of 1.03 g/mL is 34.37, while that at 300 °C and at 0.74 g/mL is 21.61. Pressures in the DAC system were totally different from 25 MPa of the flow experiment. The initial pressure in the DAC

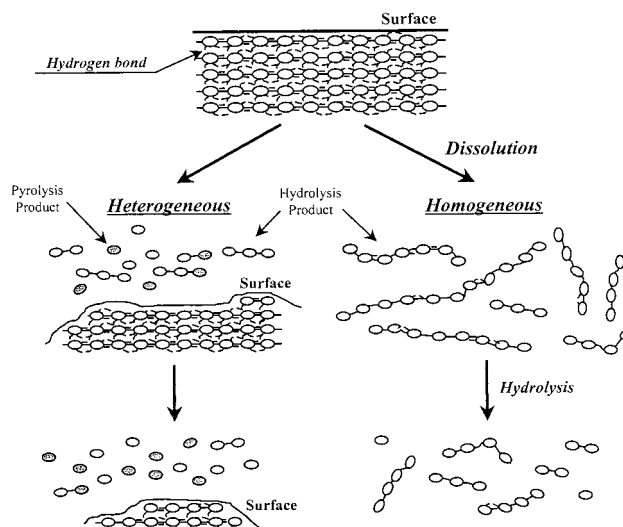


Figure 8. Cellulose reaction pathways of both a heterogeneous reaction and a homogeneous reaction.

experiment at room temperature was 60 MPa. The system pressure was elevated with increasing temperature and estimated to be 600 MPa at 300 °C, by assuming the same water density (1.03 g/mL).

Because of the difference of the reaction conditions or other effects, a clear conclusion cannot be deduced. However, as described above, the dissolution of cellulose or high-DP hydrolyzed oligomers into high-temperature water is supposed to be a possible reason for explaining the obtained results.

Conclusions

We conducted the cellulose decomposition experiments in subcritical and supercritical water and evaluated the product distribution and the cellulose decomposition rates. The following results were obtained.

(1) At 400 °C, the hydrolysis product yield was 76.5% at a cellulose conversion of almost 100% and much higher than that at 320 and 350 °C.

(2) The cellulose disappearance rate drastically increased above 350 °C.

(3) The hydrolyzed oligomers that had high DPs and, thus, were insoluble in water at low temperature were solubilized in high-temperature water at 400 °C and 25 MPa.

(4) The direct observation of the reaction field by DAC experiments showed that the cellulose disappeared with a more than 2 orders of magnitude faster rate at 300–320 °C than that estimated from the lower temperature data and with increasing transparency.

These results indicate that cellulose dissolves in high-temperature water because of the cleavage of hydrogen linkages in cellulose crystals. Thus, as shown in Figure 8, the homogeneous hydrolysis atmosphere is formed in high-temperature water and results in the drastic changes of product distributions and of the cellulose hydrolysis rate of cellulose around the critical temperature.

Acknowledgment

The authors are thankful for Grants in Aid for Scientific Research on Priority Areas (0621402 and 0423803) and for General Scientific Research (07455433)

of the Ministry of Education, Science and Culture, NEDO, and RITE.

Nomenclature

F = flow rate of the reaction solution [g/min]
 k = cellulose hydrolysis rate constant [1/s]
 k_s = cellulose shrinking rate constant [$\mu\text{m/s}$]
 L = length of a cellulose molecule [μm]
 P = reaction pressure [MPa]
 S_i = product selectivity of component i [C %]
 T_R = reaction temperature [$^{\circ}\text{C}$]
 V = reactor volume [mL]
 W_0 = amount of cellulose initially fed [g]
 W = amount of solid residue [g]
 W_i = amount of product i [g]
 X = cellulose conversion [C %]
 Y_i = product yield of component i [C %]

Products

CT = cellotriose (3-mer of glucose)
 CB = cellobiose (2-mer of glucose)
 Glc = glucose
 Fru = fructose
 GA = glyceraldehyde
 DA = dihydroxyacetone
 AG = 1,6-anhydroglucose
 Ery = erythrose
 PA = pyruvaldehyde
 HMF = 5-(hydroxymethyl)-2-furaldehyde

Greek letter

τ = residence time in the reactor [s]

Literature Cited

- (1) Townsend, S. H.; Abraham, M. A.; Huppert, G. L.; Klein, M. T.; Paspec, S. C. Solvent Effects during Reactions in Supercritical Water. *Ind. Eng. Chem. Res.* **1988**, *27*, 143–149.
- (2) Penninger M. L.; et al. *ACS Symp. Ser.* **1989**, *406*, 242.
- (3) Klein, M. T.; Torry, L. A.; Wu, B. C.; Townsend, S. H. Hydrolysis in supercritical water: Solvent effects as a probe of the reaction mechanism. *J. Supercrit. Fluids* **1990**, *3*, 222–227.

- (4) Antal, M. J., Jr.; Mok, W. S. L. Mechanism of Formation of 5-(Hydroxymethyl)-2-Furaldehyde from D-Fructose and Sucrose. *Carbohydr. Res.* **1990a**, *199*, 91–110.
- (5) Antal, M. J., Jr.; Mok, W. S. L. Four-Carbon Model Compounds for the Reactions of Sugars in Water at High Temperature. *Carbohydr. Res.* **1990b**, *199*, 111–115.
- (6) Adschiri, T.; Hirose, S.; Malaluan, R. M.; Arai, K. Uncatalytic Conversion of Cellulose in Subcritical and Supercritical Water. *J. Chem. Eng. Jpn.* **1993**, *26* (6), 676–680.
- (7) Malaluan, R. M. A Study on Cellulose Decomposition in Subcritical and Supercritical Water. Ph.D. Dissertation, Tohoku University, Sendai, Japan, 1995.
- (8) Sasaki, M.; Bernard, M. K.; Malaluan, R. M.; Hirose, S.; Takeda, N.; Adschiri, T.; Arai, K. Cellulose in Subcritical and Supercritical Water. *J. Supercrit. Fluids* **1998**, *13*, 261–268.
- (9) Kabyemela, B. M.; Adschiri, T.; Malaluan, R. M.; Arai, K. Kinetics of Glucose Epimerization and Decomposition in Subcritical and Supercritical Water. *Ind. Eng. Chem. Res.* **1997**, *36* (5), 1552–1558.
- (10) Bassett, W. A.; Shen, A. H.; Bucknum, M. A. New Diamond Anvil Cell for Hydrothermal Studies to 2.5 GPa and from -190 to 1200°C . *Rev. Sci. Instrum.* **1993**, *64* (8), 2340–2345.
- (11) Fang, Z.; Smith, R. L., Jr.; Inomata, H.; Arai, K. Phase behavior and reaction of poly(ethylene terephthalate)–water systems at pressures up to 173 MPa and temperatures up to 490°C . **1999**, *15*, 229–243.
- (12) Holgate, H. R. Oxidation Chemistry and Kinetics in Supercritical Water: Hydrogen, Carbon Monoxide, and Glucose. Ph.D. Dissertation at the Massachusetts Institute of Technology, Cambridge, MA, 1993.
- (13) Kabyemela, B. M.; Adschiri, T.; Malaluan, R. M.; Arai, K. Glucose and Fructose Decomposition in Subcritical and Supercritical Water: Detailed Reaction Pathway, Mechanisms, and Kinetics. *Ind. Eng. Chem. Res.* **1999**, *38* (8), 2888–2895.
- (14) Kabyemela, B. M.; Takigawa, M.; Adschiri, T.; Malaluan, R. M.; Arai, K. Mechanism and Kinetics of Cellobiose Decomposition in Sub- and Supercritical Water. *Ind. Eng. Chem. Res.* **1998**, *37* (2), 357–361.

Received for review September 17, 1999

Revised manuscript received May 20, 2000

Accepted June 4, 2000

IE990690J